Exciton trapping in magnetic wire structures

2001 J. Phys.: Condens. Matter 13 3283

(http://iopscience.iop.org/0953-8984/13/14/305)

INSTITUTE OF PHYSICS PUBLISHING JOURNAL OF PHYSICS: CONDENSED MATTER

J. Phys.: Condens. Matter **13** (2001) 3283–3295 www.iop.org/Journals/cm PII: S0953-8984(01)16722-6

Exciton trapping in magnetic wire structures

J A K Freire[1,3], F M Peeters[1], V N Freire[2] and G A Farias[2]

[1] Departement Natuurkunde, Universiteit Antwerpen (UIA), Universiteitsplein 1, B-2610 Antwerpen, Belgium
[2] Departamento de Física, Universidade Federal do Ceará, Centro de Ciências, Caixa Postal 6030, Campus do Pici, 60455-760 Fortaleza, Ceará, Brazil

E-mail: alking@fisica.ufc.br (J A K Freire) and peeters@uia.ua.ac.be (F M Peeters)

Received 31 August 2000

Abstract

The lateral magnetic confinement of quasi-two-dimensional excitons into wire-like structures is studied. Spin effects are taken into account and two different magnetic field profiles are considered, which can be created experimentally by the deposition of a ferromagnetic stripe on a semiconductor quantum well with magnetization parallel or perpendicular to the growth direction of the well. We find that it is possible to confine excitons into one-dimensional (1D) traps. We show that the dependence of the confinement energy on the exciton wave vector, which is related to its free direction of motion along the wire direction, is very small. Through the application of a background magnetic field it is possible to move the position of the trapping region towards the edge of the ferromagnetic stripe or even underneath the stripe. The exact position of this 1D exciton channel depends on the strength of the background magnetic field and on the magnetic polarization direction of the ferromagnetic film.

1. Introduction

Lateral localization of excitons in semiconductor quantum wells has been a focus of theoretical and experimental research in the last few years. Such one-dimensional traps can be realized, e.g., by using nonhomogeneous stress to induce a hydrostatic expansion which creates an energy minimum for the excitons [1]. Another method is to apply 1D spatially varying electrical potentials in the plane of the quantum well and to use the quantum-confined Stark effect in order to create a minimum in the exciton effective potential [2–4]. Recent theoretical [5, 6] studies on exciton confinement have shown the feasibility of achieving exciton trapping by using circular (two-dimensional) magnetic traps.

Due to recent advances in the design and manufacture of microstructured magnetic potentials [7], several works have been published on the study of magnetic barriers and magnetic superlattices. However, the majority of these experimental and theoretical investigations

[3] Permanent address: Departamento de Física, Universidade Federal do Ceará, Centro de Ciências, Caixa Postal 6030, Campus do Pici, 60455-760 Fortaleza, Ceará, Brazil.

0953-8984/01/143283+13$30.00

study the influence of such magnetic potentials on the properties of charged particles, e.g., electrons [8–11].

In this work, we propose a natural extension of such magnetic systems: the confinement of excitons in linear magnetic traps or magnetic wire structures. This paper is structured as follows. Section 2 gives a brief description of the magnetic wire structures. The theoretical model for the description of the exciton motion in a quantum well in the presence of linear magnetic traps is given in section 3. Discussion of the numerical results follows in section 4. As an example, we show the results for GaAs/Al_xGa_{1-x}As quantum wells. Finally, a summary of our results is presented in section 5.

2. Modelling the magnetic wire structures

Magnetic confinement potentials can be created by depositing ferromagnetic stripes on top of a semiconductor quantum well. An additional external homogeneous magnetic field can be applied to the system in order to maximize the confinement. A sketch of the experimental set-up is shown in figure 1(a), and a schematic cross section of the stripe with perpendicular and in-plane magnetization can be seen on the left and right sides of figure 1(b), respectively. In this system, only the z-component of the magnetic field is responsible for the magnetic modulation, and can be calculated through Coulomb's law [9].

The corresponding equation for the z-component of the magnetic field, assuming a stripe with magnetization perpendicular to the xy-plane, located at $x \in (-a/2, a/2)$, $y \in (-\infty, \infty)$, and $z \in (-h/2, h/2)$, where a (h) is the stripe width (thickness), can be written as follows:

$$B_z(x) = B_a + \frac{\mu_0 \mathcal{M}}{2\pi} [B_*(x, z + h/2) - B_*(x, z - h/2)] \tag{1a}$$

where

$$B_*(x, z) = \left[\arctan\left(\frac{x + a/2}{z}\right) - \arctan\left(\frac{x - a/2}{z}\right)\right]. \tag{1b}$$

For a stripe with in-plane magnetization the corresponding result is

$$B_z(x) = B_a + \frac{\mu_0 \mathcal{M}}{2\pi} [B_*(x + a/2, z) - B_*(x - a/2, z)] \tag{1c}$$

where

$$B_*(x, z) = \frac{1}{2} \ln\left(\frac{x^2 + (z + h/2)^2}{x^2 + (z - h/2)^2}\right). \tag{1d}$$

In the above equations, z is the distance from the centre of the stripe to the middle of the quantum well, $\mathcal{M}$ is the stripe magnetization, and B_a is the uniform applied magnetic field. The corresponding magnetic field for the stripe with perpendicular (solid curve) and in-plane (dashed curve) magnetization is shown in figure 1(c). Notice that, in the case of a perpendicular magnetization, the exciton will experience a positive effective magnetic field underneath the stripe and a negative one elsewhere as sketched on the left-hand side of figure 1(b) (see also the solid curve in figure 1(c)). The situation is completely different for the stripe with in-plane magnetization, where now the effective magnetic field has a negative peak in the region near the edge of the stripe which corresponds to the direction of $\mathcal{M}$ (at $x = a/2$) and a positive peak near the other (at $x = -a/2$) edge (see the right-hand side of figure 1(b) and the dashed curve in figure 1(c)).

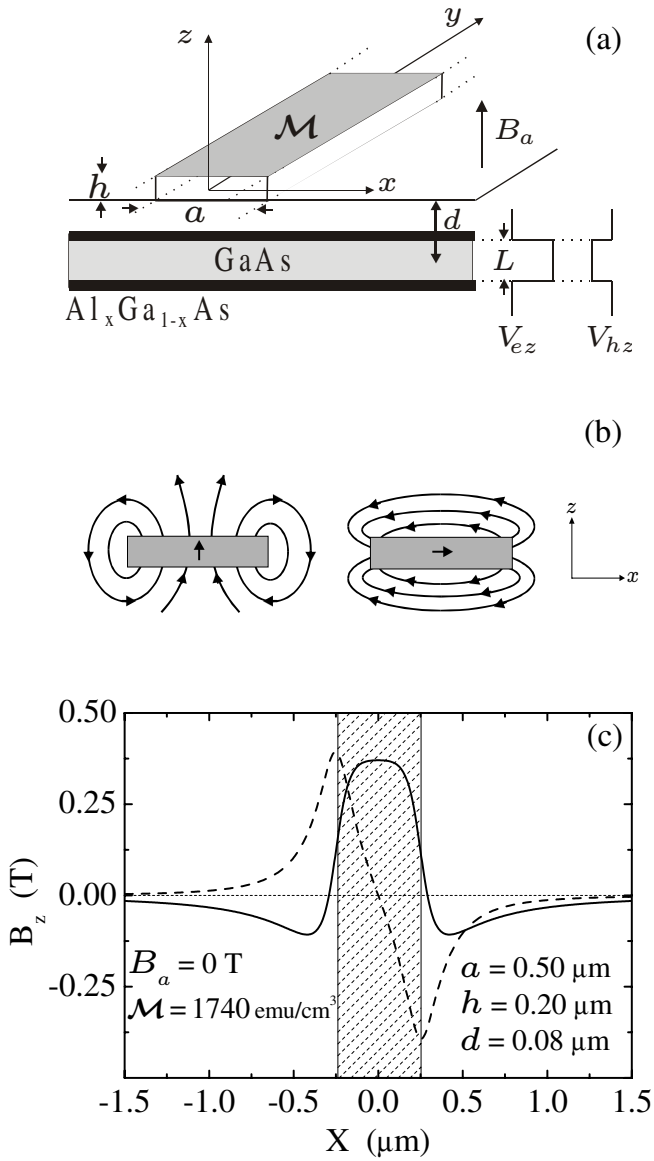

Figure 1. (a) A sketch of the experimental configuration showing the structural parameters: the stripe width a, the thickness h, and the distance from the stripe to the middle of the quantum well d. The applied magnetic field is B_a, the stripe magnetization $\mathcal{M}$, and the well width L. (b) A schematic cross section of the stripe together with the magnetic field lines for magnetization perpendicular and parallel to the x-direction. (c) A magnetic field profile corresponding to the stripe with perpendicular (——) and parallel (- - - -) magnetization. The shaded area shows the position of the magnetic stripe.

3. Theoretical model

The effective Hamiltonian describing the exciton motion in a quantum well in a nonhomogeneous magnetic field, with isotropic electron and heavy-hole effective masses m_e^* and m_h^*,

respectively, can be written in the following way:

$$H = H^{\perp}(z_e, z_h) + W(r, z_e, z_h) + H^{2D}(\boldsymbol{R}, \boldsymbol{r}) + H^{m_z}(X) \tag{2a}$$

where

$$H^{\perp}(z_e, z_h) = -\frac{\hbar^2}{2m_e^*}\frac{\partial^2}{\partial z_e^2} + V_e(z_e) - \frac{\hbar^2}{2m_h^*}\frac{\partial^2}{\partial z_h^2} + V_h(z_h) \tag{2b}$$

is the Hamiltonian describing the electron and heavy-hole confinement in the quantum well, i.e., in the z-direction;

$$W(r, z_e, z_h) = \frac{\gamma e^2}{\varepsilon r} - \frac{e^2}{\varepsilon\sqrt{r^2 + (z_e - z_h)^2}} \tag{2c}$$

is related to the difference between the 2D and 3D Coulomb interaction and is treated as a perturbation, where γ is a variational parameter which is chosen such that it minimizes $W(r, z_e, z_h)$, as discussed in detail elsewhere [12];

$$\begin{aligned} H^{2D}(\boldsymbol{R}, \boldsymbol{r}) = {} & \frac{\hbar^2}{2m_e^*}\left\{-\mathrm{i}\frac{m_e^*}{M}\boldsymbol{\nabla}_R - \mathrm{i}\,\boldsymbol{\nabla}_r + \frac{e}{\hbar c}A\left(X + \frac{m_h^*}{M}x\right)\boldsymbol{e}_y\right\}^2 \\ & + \frac{\hbar^2}{2m_h^*}\left\{-\mathrm{i}\frac{m_h^*}{M}\boldsymbol{\nabla}_R - \mathrm{i}\,\boldsymbol{\nabla}_r - \frac{e}{\hbar c}A\left(X - \frac{m_e^*}{M}x\right)\boldsymbol{e}_y\right\}^2 - \frac{\gamma e^2}{\varepsilon r} \end{aligned} \tag{2d}$$

describes the exciton motion in the xy-plane in a nonhomogeneous magnetic field, which is described by the vector potential in the Landau gauge $\boldsymbol{A}(\boldsymbol{R}) = A_Y(X)\boldsymbol{e}_Y$. In writing the above equation, we introduced the exciton relative- and centre-of-mass-motion coordinates, $\boldsymbol{r} = \boldsymbol{r}_e - \boldsymbol{r}_h$ and $\boldsymbol{R} = (m_e^*\boldsymbol{r}_e + m_h^*\boldsymbol{r}_h)/M$, respectively, with the total exciton mass $M = (m_e^* + m_h^*)$. Finally, the last term in equation (2*a*), i.e.,

$$H^{m_z}(X) = \mu_B\left[g_{e,z}S_{e,z} - \frac{1}{3}g_{h,z}J_{h,z}\right]B_z(X) - \frac{2}{3}\sum_{i=1}^{3}c_i S_{e,i}J_{h,i} \tag{2e}$$

is the Hamiltonian describing the exciton spin interaction with the nonhomogeneous magnetic field, which is oriented along the z-direction. We consider here that the contribution of the spin interaction with the in-plane magnetic field is very small and can be neglected [13, 14]. In writing down the above spin Hamiltonian, the adiabatic approximation was used, which assumes that the relative motion is fast as compared to the centre-of-mass motion. This allows us to expand the magnetic field to zero order in the relative-motion coordinate [6]. In equation (2*e*), $\mu_B = e\hbar/2m_{e,\parallel}^* c$ is the Bohr magneton, $m_z = S_{e,i} + J_{h,i}$ is the total exciton spin quantum number, which is related to the electron ($S_{e,i} = \pm 1/2$) and heavy-hole ($J_{h,i} = \pm 3/2$) spin quantum numbers, c_i is the spin–spin coupling constant related to the zero-field spin interaction, and $g_{e,z}$, $g_{h,z}$ are the z-components of the electron and heavy-hole g-factors, respectively [14].

Following the approach of Freire *et al* [5], the $H^{2D}(\boldsymbol{R}, \boldsymbol{r})$ Hamiltonian (see equation (2*d*)) can be simplified by using a transformation of the wave function analogous to the one used in the homogeneous magnetic field case, which assumes the existence of an exact integral of motion, namely the magnetic centre-of-mass momentum [15]:

$$\Psi^{m_z}(\boldsymbol{R}, \boldsymbol{r}, z_e, z_h) \Rightarrow \exp\left[-\frac{\mathrm{i}e}{\hbar c}yA_Y(X)\right]\Psi^{m_z}(\boldsymbol{R}, \boldsymbol{r}, z_e, z_h). \tag{3}$$

Further, we can use the adiabatic approximation to expand the vector potential up to the second order in the relative-motion coordinates, i.e.,

$$A_Y\left(X \pm \frac{m_{h\,(e)}^*}{M}x\right) = A_Y(X) \pm \frac{m_{h\,(e)}^*}{M}xB_z(X). \tag{4}$$

Inserting equations (3) and (4) into equation ($2d$), the H^{2D} Hamiltonian can be separated into relative- and centre-of-mass-motion Hamiltonians, i.e.,

$$H^{2D}(\boldsymbol{R}, \boldsymbol{r}) = H^{rel}(\boldsymbol{r}, \boldsymbol{R}, \boldsymbol{\nabla}_R) + H^{CM}(\boldsymbol{R})$$

with

$$H^{rel}(\boldsymbol{r}, \boldsymbol{R}, \boldsymbol{\nabla}_R) = -(\hbar^2/2\mu)\nabla_r^2 - (\gamma e^2/\varepsilon r) + u_1 + u_2$$

where

$$\begin{aligned} u_1 &= -\frac{\mathrm{i}e\hbar}{\mu c}\xi B_z(X)x\,\frac{\partial}{\partial y} - \frac{\mathrm{i}e\hbar}{Mc}\left(B_z(X)\,\frac{\partial}{\partial Y}\right)x + \frac{\mathrm{i}e\hbar}{Mc}\left(\frac{\partial}{\partial X}B_z(X) + B_z(X)\,\frac{\partial}{\partial X}\right)y \\ u_2 &= \frac{e^2}{2Mc^2}B_z(X)^2\left(\frac{\xi^2 M}{\mu}x^2 + r^2\right) \end{aligned} \tag{5}$$

and $H^{CM}(\boldsymbol{R}) = -(\hbar^2/2M)\nabla_R^2$. Here, $\mu = m_e^* m_h^*/M$ is the exciton reduced mass, and $\xi = (m_h^* - m_e^*)/M$. The procedure used to go from equation ($2d$) to equation (5) is analogous to the one used in our previous work (see equations (1)–(7) in reference [5]) on the trapping of excitons in circular magnetic traps.

To find the eigenvalues of the Hamiltonian, equation ($2a$), we use the adiabatic approximation to decouple the exciton centre-of-mass motion, which is slow, from the exciton relative motion, which is fast. We already assumed that the spin degrees of freedom depend only on the centre-of-mass coordinates. Thus, the total exciton wave function becomes a product of the wave function of the decoupled motions:

$$\Psi^{m_z}(\boldsymbol{R}, \boldsymbol{r}, z_e, z_h) = \varphi(\boldsymbol{R})\Phi(\boldsymbol{r})F(z_e, z_h)\mathcal{L}^{m_z}(\boldsymbol{R}). \tag{6}$$

The energy of the exciton confinement in the quantum well (z-direction), i.e., the eigenvalue of $\{H^{\perp}(z_e, z_h) - E^{\perp}\}F(z_e, z_h) = 0$, does not depend on the magnetic field and therefore will not contribute to the magnetic exciton trapping energy. Therefore, this energy does not have to be calculated explicitly. In order to solve the variational equation $\partial\Delta E'/\partial\gamma = 0$, with

$$\Delta E' = \langle\Phi(\boldsymbol{r})F(z_e, z_h)|W(r, z_e, z_h)|\Phi(\boldsymbol{r})F(z_e, z_h)\rangle$$

to calculate γ we follow the same procedure as described in our previous work [6].

The eigenvalues and eigenfunctions of the equation for the exciton relative motion $\{H^{rel}(\boldsymbol{r}, \boldsymbol{R}, \boldsymbol{\nabla}_R) - E^{rel}\}\Phi(\boldsymbol{r}) = 0$ are calculated using a perturbation technique, i.e., all of the B-dependent terms (see u_1 and u_2 in equation (5)) are treated as perturbations. A full discussion of the calculation method for the relative-motion energy is given in reference [5] and will not be repeated here. The spin energies can be easily calculated. The eigenvalues of $\{H^{m_z}(X) - E^{m_z}\}\mathcal{L}^{m_z}(\boldsymbol{R}) = 0$ can be written as [6]

$$E^{m_z} = \pm\frac{1}{2}\mu_B\left[(-1)^{m_z+1}g_{e,z} + g_{h,z}\right]B_z(X).$$

In writing E^{m_z}, we neglected the terms which do not depend on the magnetic field ($\pm c_z/2$), and the terms with c_x and c_y cancel because of symmetry considerations. The different signs in the above spin energy are related to the total spin quantum number $m_z = \pm 1$ (which is connected with the $\sigma^{\pm}$ polarized states) and $m_z = \pm 2$ (which is related to the dark excitons) [13]. In this work, the $m_z = \pm 2$ states will not be considered because they are not optically active.

Finally, we obtain the following Schrödinger-like equation for the exciton centre-of-mass motion:

$$\left\{-\frac{\hbar^2}{2}\,\frac{\mathrm{d}}{\mathrm{d}X}\left[\frac{1}{M^{eff}(X)}\,\frac{\mathrm{d}}{\mathrm{d}X}\right] + V^{eff}(X) - E\right\}\psi(X) = 0. \tag{7a}$$

The above equation includes the different eigenvalues for the fast motion which contribute to an effective potential and also results in a spatially dependent effective mass:

$$M^{eff}(X)/M = \left[1 - \frac{e^2\mu}{\hbar^2 M^2 c^2}\frac{\alpha_{m_r}^{n_r}}{\gamma^4}B_z(X)^2\right]^{-1} \tag{7b}$$

$$V^{eff}(X) = \frac{\hbar^2}{2M^{eff}(X)}Q_Y^2 + \frac{e^2\zeta}{2\mu c^2}\frac{\beta_{m_r}^{n_r}}{\gamma^2}B_z(X)^2 + \frac{e\hbar}{2\mu c}\xi B_z(X)m_r \pm \frac{1}{2}\mu_B\left[(-1)^{m_z+1}g_{e,z} + g_{h,z}\right]B_z(X). \tag{7c}$$

We decoupled the wave function of the centre-of-mass motion assuming that $\varphi(\boldsymbol{R}) = \exp(\mathrm{i}Q_Y Y)\psi(X)$, where Q_Y is the wave vector of the centre-of-mass motion in the Y-direction (free direction in the wire). Here, $\alpha_{m_r}^{n_r}$ and $\beta_{m_r}^{n_r}$ (in units of a_B^{*4} and a_B^{*2}, respectively) are constants related to the relative radial (n_r) and angular (m_r) quantum numbers [5], and $\zeta = (m_e^{*2} + m_h^{*2})/M$. Notice that in contrast to the case of exciton trapping through 1D scalar potentials created by an electric field [2], the effective potential for linear magnetic traps depends on the exciton wave vector Q_Y (see the first term in equation (7*c*)). The main contribution for the exciton confinement is given by the last two terms in the effective potential equation (7*c*), which are the orbital and spin Zeeman terms, respectively. The latter is a sensitive function of the exciton g-factor [14]. The diamagnetic contribution for the exciton effective potential (see second term in equation (7*c*)) contains the contribution of the well confinement through the parameter γ, which can be very important for exciton trapping when the orbital and the spin contribution are negligible, i.e., when the exciton angular momentum is zero and the exciton g-factor is small [6].

4. Exciton trapping

The trapping energy is defined as the difference in exciton energy for an exciton in a homogeneous applied field B_a and the corresponding state in the nonhomogeneous magnetic field. For our numerical calculations we used the following parameters for the ferromagnetic stripe: width $a = 0.50$ μm, thickness $h = 0.20$ μm, distance from the centre of the quantum well $d = 0.08$ μm, and the value of the stripe magnetization corresponding to iron $\mathcal{M} = 1740$ emu cm^{-3} [10, 16]. We used for the GaAs/$Al_{0.3}Ga_{0.7}$As quantum well an effective mass $m_e^* = 0.067m_0$ for electrons and $m_h^* = 0.34m_0$ for heavy holes (m_0 is the free-space electron mass), and the GaAs dielectric constant $\varepsilon = 12.53$. The different g-factors are taken from reference [14] and depend on the width of the GaAs quantum well.

The effective potential and the corresponding effective mass for the exciton confinement (see equations (7*c*) and (7*b*), respectively) for the exciton 1s ground state are shown in figure 2(a) as functions of the centre-of-mass X-coordinate for the stripe with perpendicular magnetization, and in figure 2(b) for the stripe with in-plane magnetization. In these figures, we took a quantum well width $L = 80$ Å, an applied magnetic field $B_a = 0.15$ T, and spin quantum numbers $m_z = -1$ (dotted curve) and $m_z = +1$ (dashed curve) for an exciton wave vector $Q_Y = 0$ μm^{-1}, and $m_z = -1$ (dashed–dotted–dotted curve), $m_z = +1$ (dashed–dotted curve) for $Q_Y = 5$ μm^{-1}. Notice that the effective potentials for $Q_Y = 0$ and $Q_Y = 5$ μm^{-1} are only slightly different, which suggests that the corresponding energies are close to each other and that the contribution of the Q_Y-dependent term to the exciton confinement potential (see the first term in equation (7*c*)) is small. Also notice that for the case of perpendicular magnetization, the effective potential for $m_z \leqslant 0$ has two minima near the edge of the magnetic stripe, which will be the position where the exciton will be magnetically trapped. For the

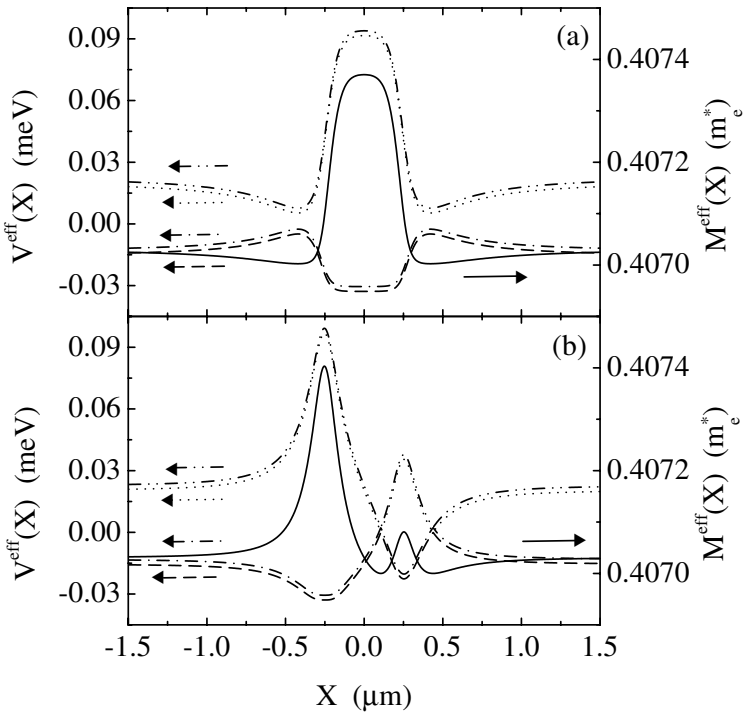

Figure 2. The effective potential for the exciton 1s ground state as a function of the centre-of-mass of the exciton X, in the case of a magnetic stripe with magnetization (a) perpendicular and (b) parallel to the X-direction. In this figure, the quantum well width is $L = 80$ Å, the applied magnetic field $B_a = 0.15$ T, the total spin quantum numbers $m_z = -1$ (· · · · · ·) and $m_z = +1$ (- - - -) for $Q_Y = 0$ μm^{-1}, and $m_z = -1$ (— · · —), $m_z = +1$ (— · —) for $Q_Y = 5$ μm^{-1}. The corresponding effective mass is also shown (——).

parallel-magnetization case and also for the perpendicular one when $m_z > 0$, the potential minimum occurs underneath the magnetic stripe and the exciton localizes exactly under the magnetic stripe. It is worthwhile to point out that for a given magnetization, the exciton spin interaction with the nonhomogeneous magnetic field can be responsible for a displacement in the minimum of the effective potential related to the different $\sigma^{\pm}$ polarized states, which is due to a change in the sign of the spin contribution (see the last term in equation (7*c*)).

The trapping energy of the exciton ground state as a function of the exciton wave vector Q_Y is shown in figure 3 for an applied field of $B_a = 0.15$ T and a well width $L = 80$ Å, for the stripe with perpendicular (figure 3(a) for $m_z = +1$ and 3(b) for $m_z = -1$) and in-plane (figure 3(c) for $m_z = +1$ and figure 3(d) for $m_z = -1$) magnetization. The trapping energy has a parabolic dispersion as expected for free-particle-like motion (see equation (7*c*)). The effect of the centre-of-mass momentum Q_Y on the exciton trapping energy is very small. Notice that the term $(\hbar^2/2M)Q_Y^2$, which does not depend on the magnetic field, is not included in the calculation of the trapping energy. Only the contribution due to the nonhomogeneous magnetic field is shown in figure 3.

Experimentally, it is very useful to control the exciton localization by means of tunable parameters, e.g., electric and magnetic fields, without the necessity of changing the structural parameters (e.g., quantum well width). For that purpose, we analysed the dependence of the exciton trapping energy under the influence of an external applied homogeneous magnetic field

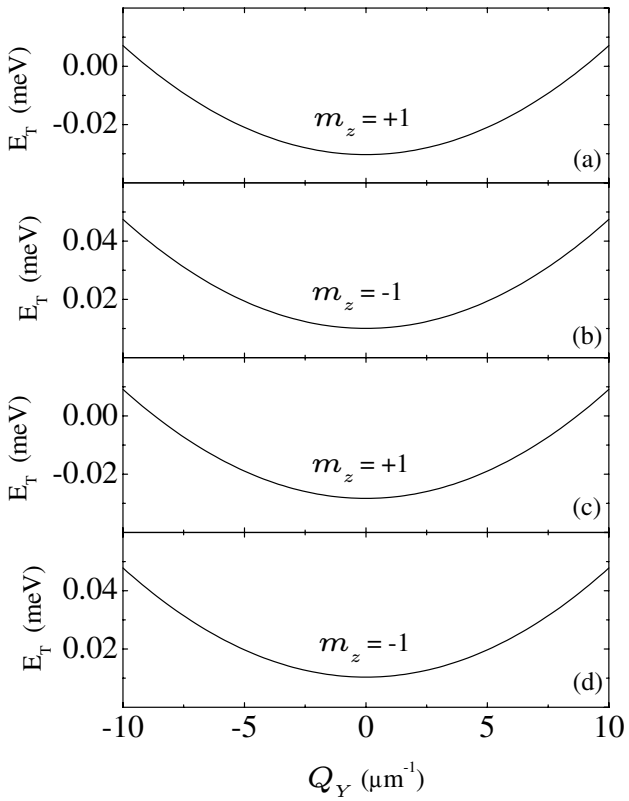

Figure 3. The contribution of the ground-state exciton trapping energy to the wave vector Q_Y-dependence for: the stripe with magnetization perpendicular to the X-axis, and spin numbers (a) $m_z = +1$ and (b) $m_z = -1$; the stripe with parallel magnetization, and spin numbers (c) $m_z = +1$ and (d) $m_z = -1$. The quantum well width $L = 80$ Å, and the applied magnetic field $B_a = 0.15$ T.

B_a, which is able to change completely the effective potential responsible for the trapping of the exciton. Figures 4 and 5 show the exciton trapping energy as a function of the applied field B_a, for the stripe with perpendicular and in-plane magnetization, respectively, for the exciton 1s ground state. Results are given for quantum well widths L of 50 Å (a), 100 Å (b), and 150 Å (c). The exciton is always trapped in the case of $m_z = +1$, except for a quantum well width $L = 100$ Å. The reason is that the corresponding exciton g-factor for this well width is almost zero [14], which greatly decreases the importance of the spin term in the effective potential expression (see equation (7c)). This is also the explanation for the large difference in magnitude (two orders in some cases) of the energy scale for $L = 50$ and 150 Å as compared to the $L = 100$ Å situation.

The trapping energy of the stripe with in-plane magnetization (figure 5) has a completely different behaviour from that of the one with perpendicular magnetization. First of all, the energy is an even function of the applied field B_a due to the functional behaviour of the corresponding nonhomogeneous magnetic field (see the dashed line in figure 1). For certain quantum well widths there exists also a critical field B_a below which the exciton is not trapped. Changing the spin quantum number from $m_z = +1$ into $m_z = -1$ drastically changes the exciton confinement dependence on the quantum well width for both magnetization directions. Using these results, one can choose an optimal situation in which the effect of the

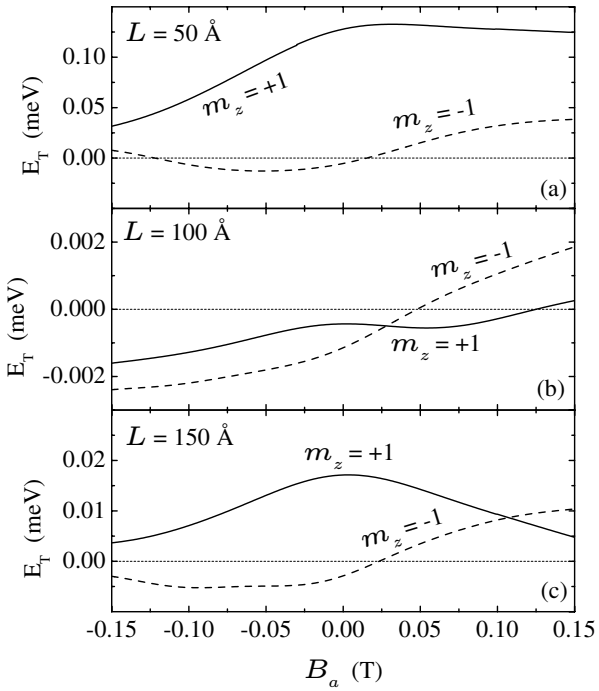

Figure 4. The trapping energy of the exciton ground state as a function of the applied magnetic field B_a for the stripe with magnetization perpendicular to the X-direction and well widths (a) $L = 50$ Å, (b) $L = 100$ Å, (c) $L = 150$ Å. The spin numbers $m_z = -1$ (- - - -) and $m_z = +1$ (——), and $Q_Y = 0\ \mu\text{m}^{-1}$.

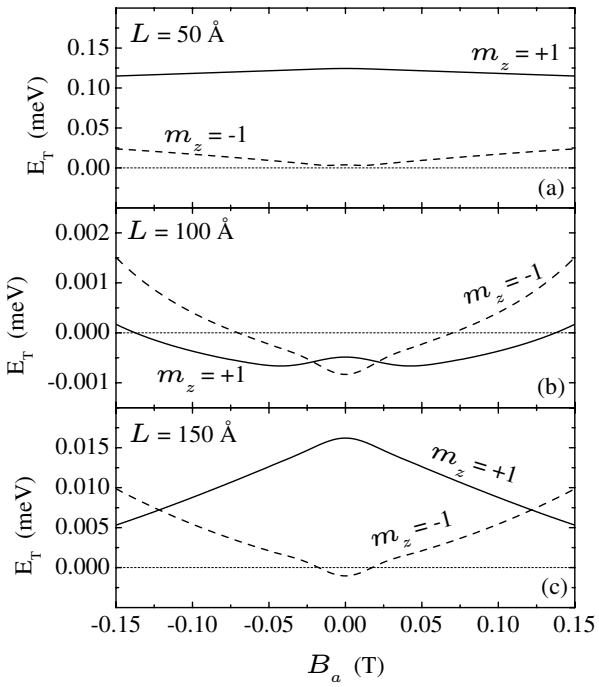

Figure 5. As figure 4, but now the stripe has magnetization parallel to the X-axis.

nonhomogeneous magnetic field on the exciton confinement is maximal and can be detected in photoluminescence (PL) experiments. By changing the applied magnetic field strength, one can modify the position of the line spectra in the PL experiments related to the $\sigma^{\pm}$ polarized states in such a way that only one of them exists (the other will be a dark state), which may make the effect of the magnetic field on the exciton confinement easier to detect.

Due to the competition between the diamagnetic interaction, the spin interaction, and the applied magnetic field, the exciton can be confined in different regions of space. This is illustrated in figures 6 and 7, where we show the wave function for the exciton ground state as a function of the X-coordinate, for the stripe with perpendicular and in-plane magnetization, respectively, for spin quantum numbers (a) $m_z = -1$ and (b) $m_z = +1$, and for different values of the applied field B_a. Notice that there is no confined exciton for the $m_z = -1$ state when $B_a = 0$, which is not the case for the $m_z = +1$ state. This can be easily explained by looking at the corresponding effective potentials (see the dotted curves in the insets of figures 6 and 7). There is no confinement region for the exciton when $m_z = -1$. Notice that for the $m_z = -1$ ($m_z = +1$) situation (see figures 6(a) and 6(b), respectively), the wave function is located near the two edges of the ferromagnetic stripe for B_a positive (negative) and underneath the stripe for B_a negative (positive). For the in-plane-magnetization situation (figure 7), the exciton is confined at one of the edges of the stripe for $m_z = -1$. Changing the sign of the background field switches the exciton from one side of the ferromagnetic edge to the other. A similar behaviour is found for $m_z = +1$ but: (i) the position of the exciton for a given B_a is at the opposite edge from the one for $m_z = -1$; and (ii) for $B_a = 0$ T, the exciton is bound and its wave function is symmetric. This magnetic field dependence is consistent with the $B_a \rightarrow -B_a$ symmetry of the binding energy (see figure 5).

5. Conclusions

We studied the behaviour of quasi-2D excitons in the presence of 1D magnetic traps. In this system, the excitons are confined into quantum wire-like states. Such linear magnetic potentials can be created experimentally by the deposition of a ferromagnetic stripe on top of a semiconductor quantum well with an additional external magnetic field applied perpendicularly to the stripe in order to maximize the exciton confinement. In this paper, we studied both possibilities for the stripe magnetization, i.e., magnetization parallel or perpendicular to the plane of the quantum well.

The main conclusions can be summarized as follows:

(i) excitons can be trapped by linear magnetic traps;
(ii) the dependence of the confinement energy on the exciton wave vector is small, but the exciton confinement is very sensitive to its spin orientation; and
(iii) the confinement of excitons in such systems can be controlled by an external tunable parameter, i.e., an applied magnetic field.

By changing the strength of the magnetic field one can move the confinement region from underneath the magnetic stripe to its edges or even to one of the edges. For the case of parallel magnetization, the external magnetic field can move the confinement region from one edge of the magnetic stripe to the other edge of the stripe. The numerical obtained trapping energies are rather small but they can be increased substantially if the amplitude of the modulated magnetic field (see figure 1(c)) is enhanced.

We also showed that the applied magnetic field can make a bright exciton becomes a dark one. This transformation is very sensitive to the quantum well width, the magnetization of

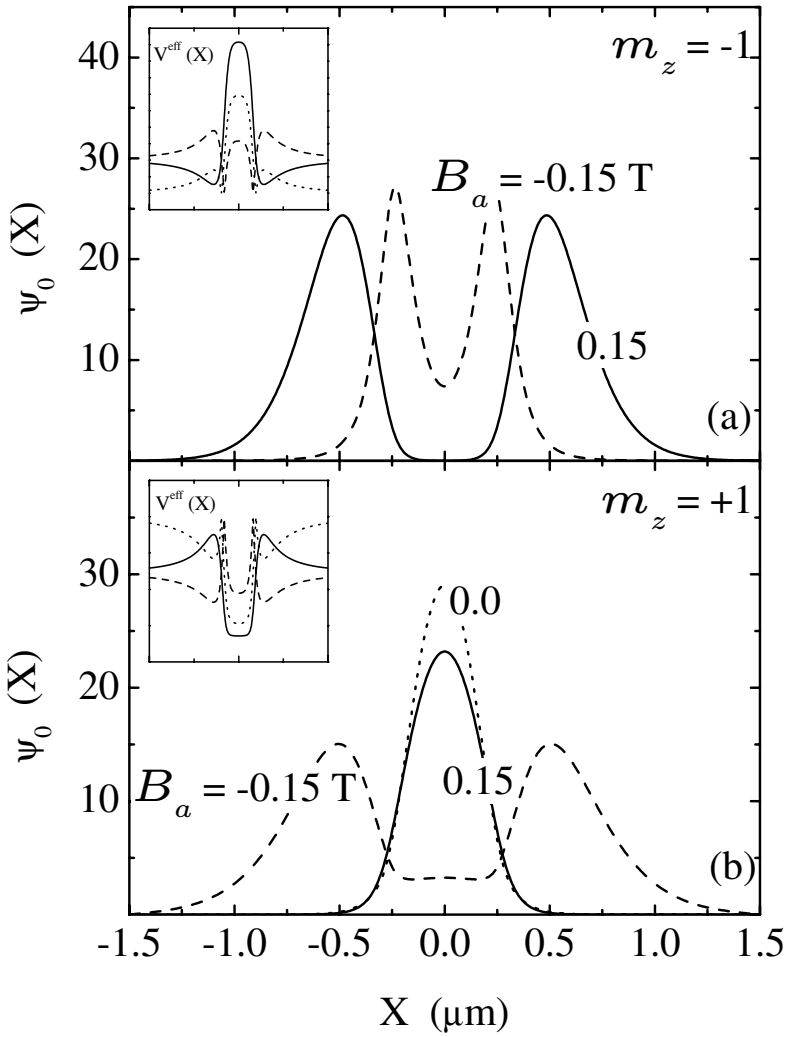

Figure 6. The wave function of the exciton ground state as a function of X, for the stripe with magnetization perpendicular to the X-direction, with spin quantum numbers (a) $m_z = -1$ and (b) $m_z = +1$. The quantum well width $L = 80$ Å, the wave vector $Q_Y = 0\ \mu\text{m}^{-1}$, and the applied magnetic field $B_a = -0.15$ T (- - - -), $B_a = 0$ T ($\cdots\cdots$), and $B_a = 0.15$ T (——). The inset shows the respective effective potentials.

the magnetic stripe, and the exciton spin contribution, i.e. through the value of the effective g-factor. Our results can help with the design of experiments to probe the exciton trapping by giving a very good estimate of the set of parameters for which the confined exciton can be detected, i.e., where the exciton is actually trapped in the magnetic wire-like confinement potential. Further, the spatial displacement of the exciton localization as controlled by changing the external applied magnetic field, from e.g. one edge of the magnetic stripe to the other, can be used experimentally to detect and analyse the effect of the nonhomogeneous magnetic field on the exciton motion. Our work is expected to provide useful insights and stimulate further developments in experimental work involving trapping of excitons in nonhomogeneous magnetic fields.

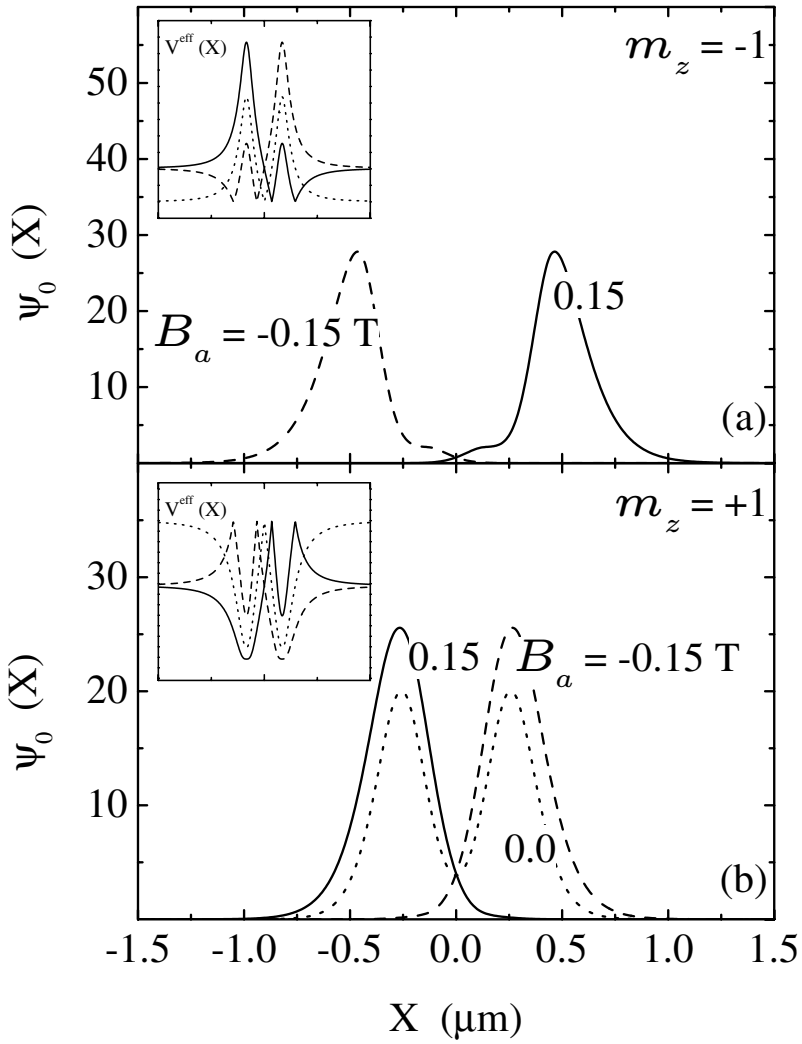

Figure 7. As figure 6, but now the stripe has magnetization parallel to the X-axis.

Acknowledgments

This research was partially supported by FWO-Vl, IUAP (Belgium), the 'Onderzoeksraad van de Universiteit Antwerpen (UIA)', and by the Inter-University Micro-Electronics Centre (IMEC, Leuven). J A K Freire was supported by the Brazilian Ministry of Culture and Education (MEC-CAPES) and F M Peeters is a research director with the FWO-Vl. V N Freire and G A Farias received financial support from the Brazilian National Research Council (CNPq) and the Brazilian Ministry of Planning through FINEP.

References

[1] Negoita V, Snoke D W and Eberl K 1999 *Appl. Phys. Lett.* **75** 2059
[2] Govorov A O and Hansen W 1998 *Phys. Rev.* B **58** 12 980

[3] Zimmermann S, Schedelbeck G, Govorov A O, Wixforth A, Kotthaus J P, Bichler M, Wegscheider W and Abstreiter G 1998 *Appl. Phys. Lett.* **73** 154
[4] Cocoletzi G H and Ulloa S E 2000 *Phys. Rev.* B **61** 13 099
[5] Freire J A K, Matulis A, Peeters F M, Freire V N and Farias G A 2000 *Phys. Rev.* B **61** 2895
[6] Freire J A K, Matulis A, Peeters F M, Freire V N and Farias G A 2000 *Phys. Rev.* B **62** 7316
[7] For a recent review see: Peeters F M and De Boeck J 1999 *Handbook of Nanostructured Materials and Nanotechnology* vol 3, ed H S Nalwa (New York: Academic) p 345
[8] Peeters F M and Matulis A 1993 *Phys. Rev.* B **48** 15 166
[9] Ibrahim I S and Peeters F M 1995 *Phys. Rev.* B **52** 17 321
[10] Nogaret A, Bending S J and Henini M 2000 *Phys. Rev. Lett.* **84** 2231
[11] Reijniers J and Peeters F M 2000 *J. Appl. Phys.* **87** 8088
[12] Wei B-H, Liu Y, Gu S-W and Yu K-W 1992 *Phys. Rev.* B **46** 4269
[13] van Kesteren H W, Cosman E C, van der Poel W A J A and Foxon C T 1990 *Phys. Rev.* B **41** 5283
[14] Blackwood E, Snelling M J, Harley R T, Andrews S R and Foxon C T B 1994 *Phys. Rev.* B **50** 14 246
[15] Gor'kov L P and Dzyaloshinsky I E 1968 *Sov. Phys.–JETP* **26** 449
[16] Kittel C 1976 *Introduction to Solid State Physics* (New York: Wiley)